Jongkil Lee
Mechanical Engineering Department
University of Utah
Salt Lake City, UT 84112

An Analytical Study of Self-Compensating Dynamic Balancer with Damping Fluid and Ball

The self-compensating dynamic balancer (SCDB) is composed of a circular disk with a groove containing ball and a low viscosity damping fluid. The equations of motion of the rotating system with SCDB were derived by the Lagrangian method. To consider dynamic stability of the motion, perturbation equations were investigated. Based on the results of stability investigation, ball positions that result in a balanced system are stable above the critical speed with small damping ($\beta' > 3.8$ case). At critical speed the perturbed motion is said to be stable for large damping ($\beta' > 2.3$ case). However, below critical speed the balls cannot stabilize the system in any case. © *1995 John Wiley & Sons, Inc.*

INTRODUCTION

The self-compensating dynamic balancer (SCDB), or automatic dynamic balancer, has been proposed in many patents to minimize the effects of rotor unbalance and vibratory forces on the rotating system during normal operation. The SCDB is usually composed of a circular disk with a groove, or race, containing spherical or cylindrical weights and a low viscosity damping fluid, although early attempts used other approaches. More automatic dynamic balancers from selected U.S. patent documents are listed in Table 1. The concept is applicable in many fields such as space vehicle components, commercial machines with rotating shafts, automobile wheels, etc.

Alexander (1964) presented the results of a theoretical analysis of an automatic dynamic balancer concept. The configuration consisted of a series of counterweights in the form of bearings mounted in races located in a long slender dynamically unbalanced spinning body. The counterweights were free to rotate with respect to the body. The basic concept of this automatic balancer was derived from an existing device for compensating for unbalanced loads in automatic washing machines with the spin-dry feature. In his simulations, the system was initially at rest and was brought to its final spin rate by the application of a torque. The lateral forces due to dynamic unbalance increase until the final spin rate is reached, and then they decay due to the action of the counterweights. However, it was not

Received October 18, 1993; Accepted September 19, 1994.

The author is now working at the Noise & Vibration Research Department of the Hyundai Heavy Industries Co., Ltd., Korea.

Shock and Vibration, Vol. 2, No. 1, pp. 59–67 (1995)

CCC 1070-9622/95/020059-09

Table 1. Selected U.S. Patents of Automatic Dynamic Balancer

Inventor	Title	Patent No.	Year
Wesley	Dynamic wheel balancer	3,346,303	1967
Mitchell	Dynamic wheel balancer	3,376,075	1968
Goodrich	Economical automatic balancer for rotating masses	3,733,923	1973
LaBarber	Vibration dampening assembly	3,799,619	1974
Cobb	Dynamic wheel and tire balancing apparatus	3,913,980	1975
Cox	Automatic and substantially permanent wheel balancing device	3,953,074	1976
Narang	Wheel and tire balancing system	4,269,451	1981
Kilgore	Dynamic rotational counterbalancer structure	4,674,356	1987

stated how the counterweights move and how this motion is related to that of the long slender body.

Many inventors have suggested various kinds of self-compensating dynamic balancer through U.S. patents, but they left it for others to explain why this system will or will not work. To the author's knowledge, the motion analysis of the balls and the rotating shaft as presented in this article represents the first attempt to analyze the dynamic stability of an SCDB with damping fluid and ball.

NONDIMENSIONAL EQUATIONS OF MOTION

A rotating shaft with SCDB carrying an unbalance disk at its midspan is shown in Figure 1. The side view of a general position of the rotating disk of mass, M, and the balls, each of mass m_i, is shown in Figure 2. The point C represents the deflected centerline of the rotating system, and the point G represents the location of the mass center of the disk. Assuming that the center C of the disk is located at the origin O of the XYZ axes when the shaft is aligned between the bearings, the lateral displacement of the shaft at the location of the disk is OC.

The equations of motion of the system can be derived by the Lagrangian method. For a circular shaft it is logical to assume that the stiffness, k, and the damping of the shaft, c, are the same regardless of the orientation of the shaft. Therefore, a scalar Lagrangian function, L, is

$$
\begin{aligned}
L = {} & \frac{1}{2} I_Z \dot{\psi}^2 + \frac{1}{2} M[\dot{X}^2 + \dot{Y}^2 - 2\varepsilon\dot{\psi}\dot{X} \sin\psi \\
& + \varepsilon^2\dot{\psi}^2 + 2\varepsilon\dot{\psi}\dot{Y}\cos\psi] \\
& + \frac{1}{2}\sum_{i=1}^{n}\left(m_i + \frac{2}{5}m_i\right)\{\dot{X}^2 + \dot{Y}^2 \\
& + (\dot{\phi}_i + \dot{\psi})^2 R^2 - 2R(\dot{\phi}_i + \dot{\psi})\,[\dot{X}\sin(\phi_i + \psi) \\
& - \dot{Y}\cos(\phi_i + \psi)]\} - \frac{1}{2}k\,(X^2 + Y^2)
\end{aligned}
\tag{1}
$$

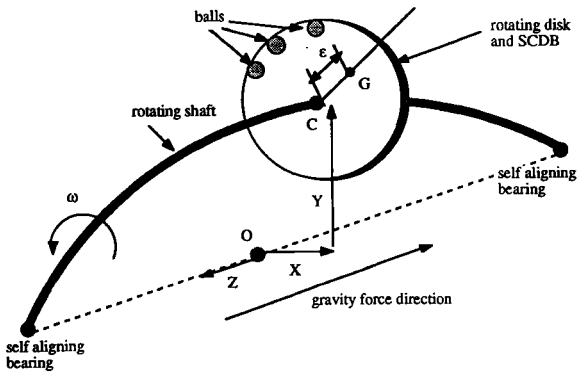

FIGURE 1 Rotating system of the SCDB.

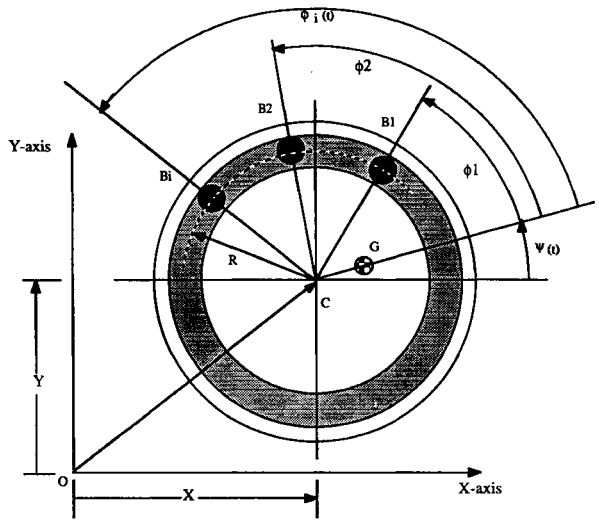

FIGURE 2 Self-compensating dynamic balancer.

where gravitational effects have been ignored. I_Z is mass moment of inertia of the disk. If the angular velocity of the disk is constant, then $\ddot{\psi} = 0$, $\dot{\psi} = \omega$, and $\psi = \omega t$ where ω is a rotation speed of the shaft. In this case equations of motion are obtained by

$$\left[1 + n\left(\frac{m}{M}\right)\right]\frac{\ddot{X}}{\omega_n^2 R} + \frac{2\zeta}{\omega_n}\frac{\dot{X}}{R} + \frac{X}{R} - \frac{\varepsilon}{R}\left(\frac{\omega}{\omega_n}\right)^2 \cos(\omega t) - \frac{1}{\omega_n^2}\frac{m}{M}\sum_{i=1}^{n}[\ddot{\phi}_i \sin(\phi_i + \omega t) + (\dot{\phi}_i + \omega)^2 \cos(\phi_i + \omega t)] = 0, \tag{2}$$

$$\left[1 + n\left(\frac{m}{M}\right)\right]\frac{\ddot{Y}}{\omega_n^2 R} + \frac{2\zeta}{\omega_n}\frac{\dot{Y}}{R} + \frac{Y}{R} - \frac{\varepsilon}{R}\left(\frac{\omega}{\omega_n}\right)^2 \sin(\omega t) + \frac{1}{\omega_n^2}\frac{m}{M}\sum_{i=1}^{n}[\ddot{\phi}_i \cos(\phi_i + \omega t) - (\dot{\phi}_i + \omega)^2 \sin(\phi_i + \omega t)] = 0, \tag{3}$$

$$\frac{\ddot{\phi}_i}{\omega_n^2} - \frac{1}{\omega_n^2}\frac{\ddot{X}}{R}\sin(\phi_i + \omega t) + \frac{1}{\omega_n^2}\frac{\ddot{Y}}{R}\cos(\phi_i + \omega t) + \frac{1}{R\omega_n^2}(\dot{\phi}_i + \omega)[\dot{X}\cos(\phi_i + \omega t) + \dot{Y}\sin(\phi_i + \omega t)] = -\beta\frac{\dot{\phi}_i}{\omega_n^2} \quad (\text{for } i = 1, 2, \ldots, n), \tag{4}$$

where,

$$\frac{m}{M} = \frac{m_i + \frac{2}{5}m_i}{M} \quad \text{and} \quad \beta = \frac{D}{\left(m_i + \frac{2}{5}m_i\right)R^2} \quad (\text{for } i = 1, 2, \ldots, n), \tag{5}$$

D is drag force on the ball per unit relative angular velocity and n is number of the balls. The natural circular frequency of the rotating system, ω_n, and the damping factor, ζ, are given by $\omega_n = \sqrt{k/M}$ and $\zeta = c/2\sqrt{kM}$, respectively. To get nondimensional equations of motion, introduce

$$t = \omega_n^{-1}\tilde{t}, \quad X = R\tilde{x}, \quad \text{and} \quad Y = R\tilde{y}, \tag{6}$$

where X, Y, and t are dimensional displacements and time and $\tilde{x}$, $\tilde{y}$, and $\tilde{t}$ are nondimensional displacements and time, respectively. Substituting Eq. (6) into the Eqs. (2), (3), and (4) then gives

$$\left[1 + n\left(\frac{m}{M}\right)\right]\ddot{\tilde{x}} + 2\zeta\dot{\tilde{x}} + \tilde{x} - \frac{\varepsilon}{R}\left(\frac{\omega}{\omega_n}\right)^2 \cos\left(\frac{\omega}{\omega_n}\tilde{t}\right) - \frac{m}{M}\sum_{i=1}^{n}\left[\ddot{\phi}_i \sin\left(\phi_i + \frac{\omega}{\omega_n}\tilde{t}\right) + \left(\dot{\phi}_i + \frac{\omega}{\omega_n}\right)^2 \cos\left(\phi_i + \frac{\omega}{\omega_n}\tilde{t}\right)\right] = 0, \tag{7}$$

$$\left[1 + n\left(\frac{m}{M}\right)\right]\ddot{\tilde{y}} + 2\zeta\dot{\tilde{y}} + \tilde{y} - \frac{\varepsilon}{R}\left(\frac{\omega}{\omega_n}\right)^2 \sin\left(\frac{\omega}{\omega_n}\tilde{t}\right) + \frac{m}{M}\sum_{i=1}^{n}\left[\ddot{\phi}_i \cos\left(\phi_i + \frac{\omega}{\omega_n}\tilde{t}\right) - \left(\dot{\phi}_i + \frac{\omega}{\omega_n}\right)^2 \sin\left(\phi_i + \frac{\omega}{\omega_n}\tilde{t}\right)\right] = 0, \tag{8}$$

$$\ddot{\phi}_i - \ddot{\tilde{x}}\sin\left(\phi_i + \frac{\omega}{\omega_n}\tilde{t}\right) + \ddot{\tilde{y}}\cos\left(\phi_i + \frac{\omega}{\omega_n}\tilde{t}\right) + \left(\dot{\phi}_i + \frac{\omega}{\omega_n}\right)\left[\dot{\tilde{x}}\cos\left(\phi_i + \frac{\omega}{\omega_n}\tilde{t}\right) + \dot{\tilde{y}}\sin\left(\phi_i + \frac{\omega}{\omega_n}\tilde{t}\right)\right] = -\beta'\dot{\phi}_i \tag{9}$$

where,

$$\beta' = \frac{\beta}{\omega_n} = \frac{D}{\left(m_i + \frac{2}{5}m_i\right)R^2\omega_n}. \tag{10}$$

STEADY SOLUTION

We will seek solutions where X and Y are zero and the balls have reached an equilibrium position. This is clearly the desired operating condition for the SCDB. When the balls are located at the equilibrium position, then

$$X = \dot{X} = \ddot{X} = 0, \quad Y = \dot{Y} = \ddot{Y} = 0, \quad \text{and} \quad \dot{\phi}_i = \ddot{\phi}_i = 0. \tag{11}$$

In this case Eqs. (2) and (3) can be expressed as

$$\frac{\varepsilon}{R}\cos(\omega t) + \frac{m}{M}\sum_{i=1}^{n}[\cos\phi_i\cos(\omega t) - \sin\phi_i\sin(\omega t)] = 0 \tag{12}$$

$$\frac{\varepsilon}{R}\sin(\omega t) + \frac{m}{M}\sum_{i=1}^{n}[\sin\phi_i\cos(\omega t) + \cos\phi_i\sin(\omega t)] = 0, \tag{13}$$

respectively. Multiplying (12) by $\cos(\omega t)$ and (13) by $\sin(\omega t)$, then adding the resulting equations, gives

$$\frac{\varepsilon}{R} + \frac{m}{M}\sum_{i=1}^{n}\cos\phi_i = 0. \tag{14}$$

Multiplying (12) by $\sin(\omega t)$ and (13) by $\cos(\omega t)$, then subtracting the resulting equations gives

$$\sum_{i=1}^{n}\sin\phi_i = 0. \tag{15}$$

Equations (14) and (15) must both be satisfied for the rotating system to be in a state of balance. According to the Eqs. (14) and (15), a rotating system is said to be in a state of balance when the result of all centrifugal forces acting on the rotating system is zero and the centrifugal forces do not give rise to any couple acting on the rotating system.

PERTURBATION EQUATIONS

To investigate the stability of the motion equations, these equations are first perturbed and the resulting equations are analyzed further to determine whether the perturbations grow or decay with time. According to this techniques, the solution is represented by the first few terms of an asymptotic expansion, usually not more than two terms. Suppose that the balls have some slight displacements from dynamic equilibrium positions, ϕ_{si} which are constants. Let

$$\phi_i = \phi_{si} + \varepsilon\phi_i + O(\varepsilon^2), \quad (\text{for } i = 1, 2, \ldots, n) \tag{16}$$

$$\tilde{x} = \tilde{x}_0 + \varepsilon\tilde{x}_1 + O(\varepsilon^2), \tag{17}$$

$$\tilde{y} = \tilde{y}_0 + \varepsilon\tilde{y}_1 + O(\varepsilon^2). \tag{18}$$

We seek approximate solutions that are uniformly valid for small ε. To simplify the Eqs. (7), (8), and (9), let

$$\frac{\omega}{\omega_n} = \tilde{\omega}, \quad \frac{\varepsilon}{R} = \tilde{R}, \quad \text{and} \quad \frac{m}{M} = \tilde{m}. \tag{19}$$

Substituting Eqs. (16), (17), (18), and (19) into the Eqs. (7), (8), and (9) then the nondimensional equations of motion are obtained as

$$\begin{aligned}&(1 + n\tilde{m})(\ddot{\tilde{x}}_0 + \varepsilon\ddot{\tilde{x}}_1) + 2\zeta(\dot{\tilde{x}}_0 + \varepsilon\dot{\tilde{x}}_1) + (\tilde{x}_0 + \varepsilon\tilde{x}_1) - \tilde{R}\tilde{\omega}^2\cos(\tilde{\omega}\tilde{t})\\ &- \tilde{m}\sum_{i=1}^{n}\{\varepsilon\ddot{\phi}_i[\sin(\phi_{si} + \tilde{\omega}\tilde{t}) + \cos(\phi_{si} + \tilde{\omega}\tilde{t})\varepsilon\phi_i]\\ &+ [\tilde{\omega}^2 + \varepsilon(2\tilde{\omega}\dot{\phi}_i + \varepsilon\dot{\phi}_i^2)][\cos(\phi_{si} + \tilde{\omega}\tilde{t}) - \varepsilon\phi_i\sin(\phi_{si} + \tilde{\omega}\tilde{t})]\} + O(\varepsilon^2) = 0,\end{aligned} \tag{20}$$

$$\begin{aligned}&(1 + n\tilde{m})(\ddot{\tilde{y}}_0 + \varepsilon\ddot{\tilde{y}}_1) + 2\zeta(\dot{\tilde{y}}_0 + \varepsilon\dot{\tilde{y}}_1) + (\tilde{y}_0 + \varepsilon\tilde{y}_1) - \tilde{R}\tilde{\omega}^2\sin(\tilde{\omega}\tilde{t})\\ &+ \tilde{m}\sum_{i=1}^{n}\{\varepsilon\ddot{\phi}_i[\cos(\phi_{si} + \tilde{\omega}\tilde{t}) - \varepsilon\phi_i\sin(\phi_{si} + \tilde{\omega}\tilde{t})]\\ &- [\tilde{\omega}^2 + \varepsilon(2\tilde{\omega}\dot{\phi}_i + \varepsilon\dot{\phi}_i^2)][\sin(\phi_{si} + \tilde{\omega}\tilde{t}) + \cos(\phi_{si} + \tilde{\omega}\tilde{t})\varepsilon\phi_i]\}\\ &+ O(\varepsilon^2) = 0,\end{aligned} \tag{21}$$

$$\begin{aligned}&\varepsilon\ddot{\phi}_i - (\ddot{\tilde{x}}_0 + \varepsilon\ddot{\tilde{x}}_1)[\sin(\phi_{si} + \tilde{\omega}\tilde{t}) + \cos(\phi_{si} + \tilde{\omega}\tilde{t})\varepsilon\phi_i]\\ &+ (\ddot{\tilde{y}}_0 + \varepsilon\ddot{\tilde{y}}_1)[\cos(\phi_{si} + \tilde{\omega}\tilde{t}) - \varepsilon\phi_i\sin(\phi_{si} + \tilde{\omega}\tilde{t})]\\ &+ (\varepsilon\dot{\phi}_i + \tilde{\omega})\{(\dot{\tilde{x}}_0 + \varepsilon\dot{\tilde{x}}_1)[\cos(\phi_{si} + \tilde{\omega}\tilde{t}) - \varepsilon\phi_i\sin(\phi_{si} + \tilde{\omega}\tilde{t})]\\ &+ (\dot{\tilde{y}}_0 + \varepsilon\dot{\tilde{y}}_1)[\sin(\phi_{si} + \tilde{\omega}\tilde{t}) + \cos(\phi_{si} + \tilde{\omega}\tilde{t})\varepsilon\phi_i]\} + O(\varepsilon^2) = -\beta'\,\varepsilon\dot{\phi}_i.\end{aligned} \tag{22}$$

Equating the coefficients of power of ε^0 and using the Eqs. (14) and (15) then gives

$$(1 + n\tilde{m})\ddot{\tilde{x}}_0 + 2\zeta\dot{\tilde{x}}_0 + \tilde{x}_0 = \tilde{R}\tilde{\omega}^2\cos(\tilde{\omega}\tilde{t}) + \tilde{m}\sum_{i=1}^{n}\tilde{\omega}^2\cos(\phi_{si} + \tilde{\omega}\tilde{t}) = \tilde{\omega}^2\left[\left(\tilde{R} + \tilde{m}\sum_{i=1}^{n}\cos\phi_{si}\right)\cos(\tilde{\omega}\tilde{t}) - \tilde{m}\sum_{i=1}^{n}\sin\phi_{si}\sin(\tilde{\omega}\tilde{t})\right] = 0, \tag{23}$$

$$(1 + n\tilde{m})\ddot{\tilde{y}}_0 + 2\zeta\dot{\tilde{y}}_0 + \tilde{y}_0 = \tilde{R}\tilde{\omega}^2\sin(\tilde{\omega}\tilde{t}) + \tilde{m}\sum_{i=1}^{n}\tilde{\omega}^2\sin(\phi_{si} + \tilde{\omega}\tilde{t}) = \tilde{\omega}^2\left[\left(\tilde{R} + \tilde{m}\sum_{i=1}^{n}\cos\phi_{si}\right)\sin(\tilde{\omega}\tilde{t}) + \tilde{m}\sum_{i=1}^{n}\sin\phi_{si}\cos(\tilde{\omega}\tilde{t})\right] = 0. \tag{24}$$

These equations are transient oscillations that decay with time. Thus the ε^0 equations have the steady solutions $\tilde{x}_0 = \tilde{y}_0 = 0$ and ϕ_{si}.

Equating coefficients of like power of ε^1 yields

$$(1 + n\tilde{m})\ddot{\tilde{x}}_1 + 2\zeta\dot{\tilde{x}}_1 + \tilde{x}_1 = \tilde{m}\sum_{i=1}^{n}\{\ddot{\phi}_i\sin(\phi_{si} + \tilde{\omega}\tilde{t}) - \tilde{\omega}^2\phi_i\sin(\phi_{si} + \tilde{\omega}\tilde{t}) + 2\tilde{\omega}\dot{\phi}_i\cos(\phi_{si} + \tilde{\omega}\tilde{t})\}, \tag{25}$$

$$(1 + n\tilde{m})\ddot{\tilde{y}}_1 + 2\zeta\dot{\tilde{y}}_1 + \tilde{y}_1 = -\tilde{m}\sum_{i=1}^{n}\{\ddot{\phi}_i\cos(\phi_{si} + \tilde{\omega}\tilde{t}) - \tilde{\omega}^2\phi_i\cos(\phi_{si} + \tilde{\omega}\tilde{t}) - 2\tilde{\omega}\dot{\phi}_i\sin(\phi_{si} + \tilde{\omega}\tilde{t})\}, \tag{26}$$

$$\begin{aligned}&\ddot{\phi}_i - \ddot{\tilde{x}}_0\phi_i\cos(\phi_{si} + \tilde{\omega}\tilde{t}) - \ddot{\tilde{x}}_1\sin(\phi_{si} + \tilde{\omega}\tilde{t}) - \ddot{\tilde{y}}_0\phi_i\sin(\phi_{si} + \tilde{\omega}\tilde{t}) + \ddot{\tilde{y}}_1\cos(\phi_{si} + \tilde{\omega}\tilde{t}) + \dot{\phi}_i\dot{\tilde{x}}_0\cos(\phi_{si} + \tilde{\omega}\tilde{t}) \\ &+ \dot{\phi}_i\dot{\tilde{y}}_0\sin(\phi_{si} + \tilde{\omega}\tilde{t}) - \tilde{\omega}\dot{\tilde{x}}_0\phi_i\sin(\phi_{si} + \tilde{\omega}\tilde{t}) + \tilde{\omega}\dot{\tilde{x}}_1\cos(\phi_{si} + \tilde{\omega}\tilde{t}) + \tilde{\omega}\dot{\tilde{y}}_0\phi_i\cos(\phi_{si} + \tilde{\omega}\tilde{t}) \\ &+ \tilde{\omega}\dot{\tilde{y}}_1\sin(\phi_{si} + \tilde{\omega}\tilde{t}) = -\beta'\dot{\phi}_i.\end{aligned} \tag{27}$$

DYNAMIC STABILITY

The perturbed equations, (25), (26), and (27) do not appear to be integrable in closed form. Therefore, to investigate the stability of the perturbed equations, it is convenient to utilize the fact that a system of n second order equations can be transformed into a system of $2n$ first order equations. Let us introduce six state variables,

$$\{\eta_1\ \ \eta_2\ \ \eta_3\ \ \eta_4\ \ \eta_5\ \ \eta_6\}^T = \{\tilde{x}_1,\ \dot{\tilde{x}}_1,\ \tilde{y}_1,\ \dot{\tilde{y}}_1,\ \phi_1,\ \dot{\phi}_1\}^T$$
$$\text{and}\ \ \{\dot{\eta}_2\ \ \dot{\eta}_4\ \ \dot{\eta}_6\}^T = \{\ddot{\tilde{x}}_1\ \ \ddot{\tilde{y}}_1\ \ \ddot{\phi}_1\}^T. \tag{28}$$

For convenience, consider only the one ball case. Therefore, using the state-space method, the perturbed equations, (2.60), can be expressed by

$$\{\dot{\eta}_1\ \ \dot{\eta}_2\ \ \dot{\eta}_3\ \ \dot{\eta}_4\ \ \dot{\eta}_5\ \ \dot{\eta}_6\}^T = [\mathbf{A}(\tilde{\mathbf{t}})]\{\eta_1\ \ \eta_2\ \ \eta_3\ \ \eta_4\ \ \eta_5\ \ \eta_6\}^T \tag{29}$$

where, the system matrix, $[\mathbf{A}(\tilde{\mathbf{t}})]$, is defined as

$$[\mathbf{A}(\tilde{\mathbf{t}})] = \begin{bmatrix} 0 & 1 & 0 & 0 & 0 & 0 \\ A_{21} & A_{22} & A_{23} & A_{24} & A_{25} & A_{26} \\ 0 & 0 & 0 & 1 & 0 & 0 \\ A_{41} & A_{42} & A_{43} & A_{44} & A_{45} & A_{46} \\ 0 & 0 & 0 & 0 & 0 & 1 \\ A_{61} & A_{62} & A_{63} & A_{64} & A_{65} & A_{66} \end{bmatrix} \tag{30}$$

and the elements of the system matrix, $[\mathbf{A}(\tilde{\mathbf{t}})]$, are expressed by

$$A_{21} = -(1 + \tilde{m})[1 + \tilde{m}\sin^2(\phi_{s1} + \tilde{\omega}\tilde{t})]/(1 + \tilde{m})^2, \tag{31}$$

$$A_{22} = [-2\zeta(1 + \tilde{m}) - 2\zeta(1 + \tilde{m})\sin^2(\phi_{s1} + \tilde{\omega}\tilde{t}) + \tilde{m}^2(1 + \tilde{m})\tilde{\omega}\sin(\phi_{s1} + \tilde{\omega}\tilde{t})\cos(\phi_{s1} + \tilde{\omega}\tilde{t}) - \tilde{m}(1 + \tilde{m})\tilde{\omega}\sin(\phi_{s1} + \tilde{\omega}\tilde{t})\cos(\phi_{s1} + \tilde{\omega}\tilde{t})]/(1 + \tilde{m})^2, \tag{32}$$

$$A_{23} = \tilde{m}(1 + \tilde{m})\sin(\phi_{s1} + \tilde{\omega}\tilde{t})\cos(\phi_{s1} + \tilde{\omega}\tilde{t})/(1 + \tilde{m})^2, \tag{33}$$

$$A_{24} = [2\zeta\tilde{m}(1 + \tilde{m})\sin(\phi_{s1} + \tilde{\omega}\tilde{t})\cos(\phi_{s1} + \tilde{\omega}\tilde{t}) - \tilde{m}(1 + \tilde{m})\tilde{\omega}\sin^2(\phi_{s1} + \tilde{\omega}\tilde{t})]/(1 + \tilde{m})^2, \tag{34}$$

$$A_{25} = [-\tilde{m}(1 + \tilde{m})\tilde{\omega}^2\sin(\phi_{s1} + \tilde{\omega}\tilde{t}) - \tilde{m}^2(1 + \tilde{m})\tilde{\omega}^2\sin(\phi_{s1} + \tilde{\omega}\tilde{t})]/(1 + \tilde{m})^2, \tag{35}$$

$$A_{26} = [2\tilde{m}(1 + \tilde{m})\tilde{\omega} \cos(\phi_{s1} + \tilde{\omega}\tilde{t}) - \tilde{m}(1 + \tilde{m})^2 \sin^2(\phi_{s1} + \tilde{\omega}\tilde{t}) - \tilde{m}\beta'(1 + \tilde{m})^2 \sin(\phi_{s1} + \tilde{\omega}\tilde{t})]/(1 + \tilde{m})^2, \quad (36)$$

$$A_{41} = -(1 + \tilde{m})\tilde{m} \sin(\phi_{s1} + \tilde{\omega}\tilde{t}) \cos(\phi_{s1} + \tilde{\omega}\tilde{t})/(1 + \tilde{m})^2, \quad (37)$$

$$A_{42} = [\tilde{m}(1 + \tilde{m})\tilde{\omega} \cos^2(\phi_{s1} + \tilde{\omega}\tilde{t}) + \tilde{m}^2(1 + \tilde{m})\tilde{\omega} \cos^2(\phi_{s1} + \tilde{\omega}\tilde{t}) - 2\tilde{m}(1 + \tilde{m})\zeta \sin(\phi_{s1} + \tilde{\omega}\tilde{t}) \cos(\phi_{s1} + \tilde{\omega}\tilde{t})]/(1 + \tilde{m})^2, \quad (38)$$

$$A_{43} = -(1 + \tilde{m})[1 - \tilde{m} \cos^2(\phi_{s1} + \tilde{\omega}\tilde{t})]/(1 + \tilde{m})^2, \quad (39)$$

$$A_{44} = [-2\zeta(1 + \tilde{m}) + 2\zeta\tilde{m}(1 + \tilde{m}) \cos^2(\phi_{s1} + \tilde{\omega}\tilde{t}) - \tilde{m}(1 + \tilde{m})\tilde{\omega} \sin(\phi_{s1} + \tilde{\omega}\tilde{t}) \cos(\phi_{s1} + \tilde{\omega}\tilde{t}) - \tilde{m}^2(1 + \tilde{m})\tilde{\omega} \sin(\phi_{s1} + \tilde{\omega}\tilde{t}) \cos(\phi_{s1} + \tilde{\omega}\tilde{t})]/(1 + \tilde{m})^2, \quad (40)$$

$$A_{45} = [\tilde{m}(1 + \tilde{m})\tilde{\omega}^2 \cos(\phi_{s1} + \tilde{\omega}\tilde{t}) - \tilde{m}^2(1 + \tilde{m})\tilde{\omega}^2 \cos(\phi_{s1} + \tilde{\omega}\tilde{t})]/(1 + \tilde{m})^2, \quad (41)$$

$$A_{46} = [-2\tilde{m}(1 + \tilde{m})\tilde{\omega} \sin(\phi_{s1} + \tilde{\omega}\tilde{t}) - \tilde{m}(1 + \tilde{m})^2 \sin(\phi_{s1} + \tilde{\omega}\tilde{t}) \cos(\phi_{s1} + \tilde{\omega}\tilde{t}) - \tilde{m}\beta'(1 + \tilde{m})^2 \cos(\phi_{s1} + \tilde{\omega}\tilde{t})]/(1 + \tilde{m})^2, \quad (42)$$

$$A_{61} = -\sin(\phi_{s1} + \tilde{\omega}\tilde{t}), \quad (43)$$

$$A_{62} = (1 + \tilde{m})\tilde{\omega} \cos(\phi_{s1} + \tilde{\omega}\tilde{t}) - 2\zeta \sin(\phi_{s1} + \tilde{\omega}\tilde{t}), \quad (44)$$

$$A_{63} = \cos(\phi_{s1} + \tilde{\omega}\tilde{t}), \quad (45)$$

$$A_{64} = -(1 + \tilde{m})\tilde{\omega} \sin(\phi_{s1} + \tilde{\omega}\tilde{t}) + 2\zeta \cos(\phi_{s1} + \tilde{\omega}\tilde{t}), \quad (46)$$

$$A_{65} = -\tilde{m}\tilde{\omega}^2, \quad (47)$$

$$A_{66} = -(1 + \tilde{m})[\beta' + \sin(\phi_{s1} + \tilde{\omega}\tilde{t})]. \quad (48)$$

However, in Eq. (27), $\ddot{x}_0$, $\ddot{y}_0$, $\dot{x}_0$, and $\dot{y}_0$ are dropped because these are transient oscillations that disappear with time.

The Floquet theory has been developed for characterizing the functional behavior of linear ordinary differential equations with periodic coefficients. In Eq. (30), $[\mathbf{A}(\tilde{\mathbf{t}})]$ is a 6×6 matrix such that $[\mathbf{A}(\tilde{\mathbf{t}} + T)] = [\mathbf{A}(\tilde{\mathbf{t}})]$ where T is period of the system matrix, $[\mathbf{A}(\tilde{\mathbf{t}})]$. To determine the eigenvalues and hence the characteristic exponents of (29), one can numerically calculate a fundamental set of solutions $[U]$. $[U]$ satisfies the matrix Eq. (29) of $[\dot{U}] = [\mathbf{A}(\tilde{\mathbf{t}})][U]$ using the initial conditions $[U(0)] = [I]$ during a period of oscillation. Then $[\mathbf{U}(\mathbf{T})]$, nonsingular constant 6×6 matrix, is obtained as

$$\begin{aligned} [U(\Delta t)] &= [I] + \Delta t[A(0)][U(0)], \\ [U(2\Delta t)] &= [U(\Delta t)] + \Delta t[A(\Delta t)][U(\Delta t)], \\ [U(3\Delta t)] &= [U(2\Delta t)] + \Delta t[A(2\Delta t)][U(2\Delta t)], \ldots, \text{ and} \\ [\mathbf{U}(\mathbf{T})] &= [U(T - \Delta t)] + \Delta t[A(T - \Delta t)][U(T - \Delta t)]. \end{aligned} \quad (49)$$

Solving the characteristic equation, $|[\mathbf{U}(\mathbf{T})] - \mu[I]| = 0$, yields a set of characteristic multipliers, that is, the characteristic roots, μ's, of the matrix $[\mathbf{U}(\mathbf{T})]$. To investigate the dynamic stability of Eq. (29), numerical simulation was carried out using the Floquet algorithm. Figures 3–8 show the results of computer simulation of the Floquet algorithm when $\tilde{\omega}$ is 1.5 (above critical speed), 1.0 (at critical speed), and 0.7 (below critical speed) with only one ball. The input data were chosen as $\tilde{m} = 0.005$, $\zeta = 0.01$, and $\phi_{s1} = \pi$. Figure 3 is a plot of the characteristic multipliers, μ's, in complex plane above critical speed ($\tilde{\omega} = 1.5$). From this figure the moduli, that is absolute values, of the characteristic multipliers are found to be a set of {0.9765, 0.9765, 0.9562, 0.9562, 0.9833, 0.9833} and all of the moduli are less than

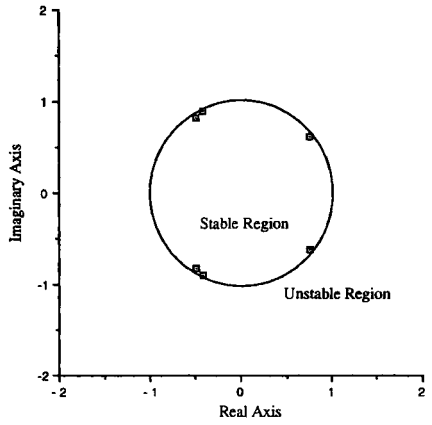

FIGURE 3 Characteristic multipliers ($\tilde{\omega} = 1.5$ and $\beta' = 0.01$ case). Characteristic multipliers: $-0.4129 \pm 0.8925i$, $0.7617 \pm 0.6116i$, and $-0.4925 \pm 0.8197i$.

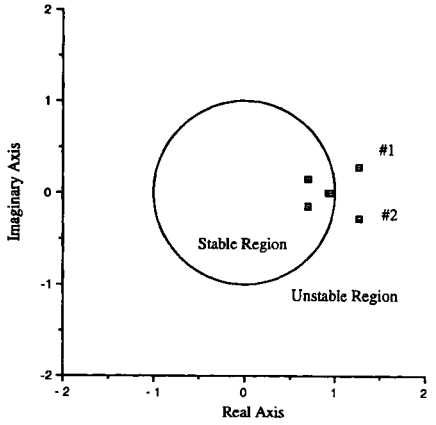

FIGURE 4 Characteristic multipliers ($\bar{\omega}$ = 1.0 and β' = 0.01 case). Characteristic multipliers: 1.2712 ± 0.2814i, 0.7028 ± 0.1435i, 0.9238, and 0.9508.

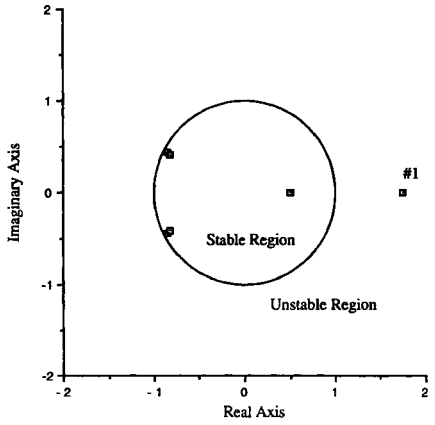

FIGURE 6 Characteristic multipliers ($\bar{\omega}$ = 0.7 and β' = 0.01 case). Characteristic multipliers: 1.7514, 0.5059, −0.8181 ± 0.4060i, and −0.8517 ± 0.4446i.

1, that is all of the moduli are inside of the unit circle. Therefore, the perturbed motion is said to be stable above critical speed when β' = 0.01. Figure 4 is a plot of the characteristic multipliers in the complex plane at critical speed ($\bar{\omega}$ = 1.0) when β' = 0.01. From this figure the moduli of the characteristic multipliers are found to be a set of {1.302, 1.302, 0.717, 0.717, 0.9238, 0.9508} and two of the moduli (#1 and #2) are greater than 1, that is #1 and #2 are outside of the unit circle. Therefore, when β' = 0.01 the perturbed motion is unstable at critical speed. Figure 5 is a plot of one of the moduli of the characteristic multipliers versus β' at critical speed ($\bar{\omega}$ = 1.0). However, from this figure increased β' can yield a stable system at critical speed. Figure 6 is a plot of the characteristic multipliers in a complex plane below critical speed ($\bar{\omega}$ < 1) when β' = 0.01. From this figure the moduli of the characteristic multipliers are given by the set {1.7514, 0.5059, 0.9133, 0.9133, 0.9607, 0.9607} and one of the moduli (#1) is greater than 1, that is, #1 is outside of the unit circle and the system is unstable. Figure 7 is a plot of one of the characteristic multipliers versus β' below critical speed ($\bar{\omega}$ = 0.9). From this figure increased β' does not appear to be able to make the system stable below critical speed. Therefore, the perturbed motion appears to be unstable below critical speed in any case. Figure 8 shows a dynamic stability diagram of the perturbed motion (β' versus $\bar{\omega}$). From this diagram the damping coefficient, β', of the fluid plays an important role in the stability of the perturbed motion.

Direct integration of the equations of motion by computer simulation offers an attractive alter-

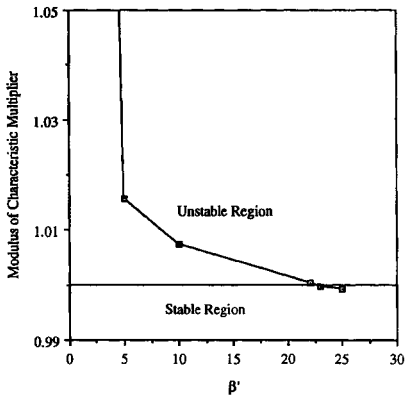

FIGURE 5 Modulus of characteristic multiplier versus β' ($\bar{\omega}$ = 1.0 case).

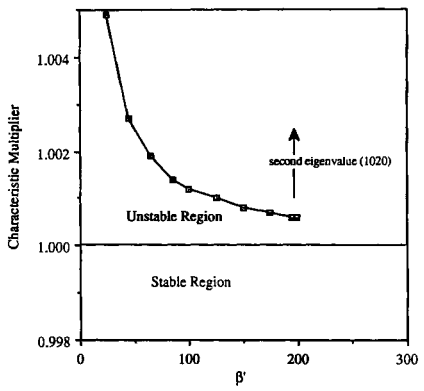

FIGURE 7 Modulus of characteristic multiplier versus β' ($\bar{\omega}$ = 0.9 case).

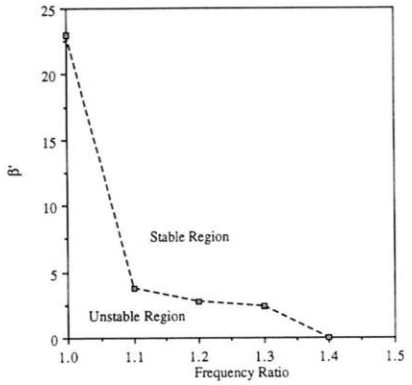

FIGURE 8 Dynamic stability diagram ($\bar{\omega}$ versus β').

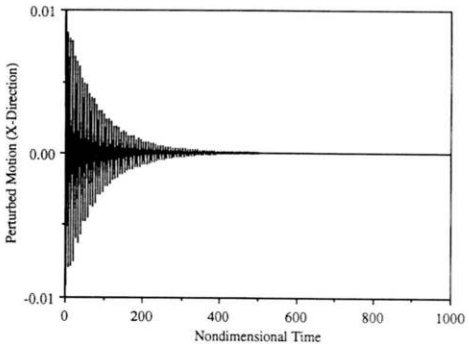

FIGURE 9 X-direction perturbation versus nondimensional time ($\bar{\omega} = 1.5$). Initial conditions: $\bar{x}_1(0) = \bar{y}_1(0) = 0.01$, $\dot{\bar{x}}_1(0) = \dot{\bar{y}}_1(0) = 0$, $\phi_{s1} = 3.13$, $\phi_{s2} = 3.15$, $\phi_1(0) = \phi_2(0) = 0.01$, $\dot{\phi}_1(0) = \dot{\phi}_2(0) = 0$, $\bar{m} = 0.005$, $\bar{R} = 0.001$, and $\beta' = .01$.

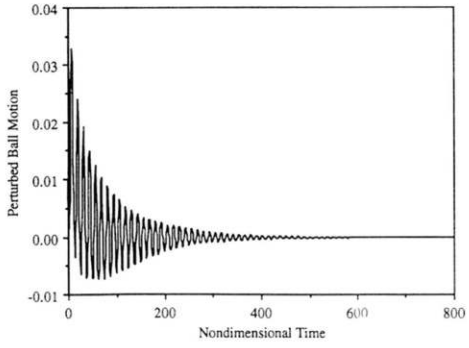

FIGURE 10 Perturbed ball motion versus nondimensional time ($\bar{\omega} = 1.5$). Initial conditions: $\bar{x}_1(0) = \bar{y}_1(0) = 0.01$, $\dot{\bar{x}}_1(0) = \dot{\bar{y}}_1(0) = 0$, $\phi_{s1} = 3.13$, $\phi_{s2} = 3.15$, $\phi_1(0) = \phi_2(0) = 0.01$, $\dot{\phi}_1(0) = \dot{\phi}_2(0) = 0$, $\bar{m} = 0.005$, $\bar{R} = 0.001$, and $\beta' = .01$.

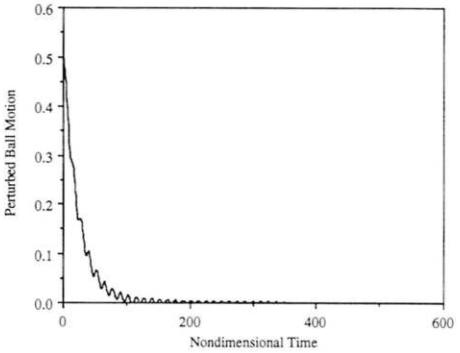

FIGURE 11 Perturbed ball motion versus nondimensional time ($\bar{\omega} = 1.5$). Initial conditions: $\bar{x}_o(0) = \bar{y}_o(0) = 0.01$, $\dot{\bar{x}}_o(0) = \dot{\bar{y}}_o(0) = 0$, $\phi_{s1} = 3.13$, $\phi_{s2} = 3.15$, $\phi_1(0) = \phi_2(0) = 0.5$, $\dot{\phi}_1(0) = \dot{\phi}_2(0) = 0$, $\bar{m} = 0.005$, $\bar{R} = 0.001$, and $\beta' = .01$.

native for the stability investigation of a general time-varying motion. Hence, to investigate perturbed motion in the dimensionless time domain the numerical method was directly applied to Eqs. (25), (26), and (27), with two balls. Figures 9–15 show results of computer simulations when $\bar{\omega}$ is 1.5 (above critical speed), 1.0 (at critical speed), and 0.7 (below critical speed). Lee (1993) selected the dynamic equilibrium positions, $\phi_{s1} = 3.13$ and $\phi_{s2} = 3.15$. Figures 9 and 10 are plots of the $\bar{x}_1(\bar{t})$ and $\phi_1(\bar{t})$ with two balls. From these figures, if after the balls in a system are given some initial motions, $\bar{x}_1(0) = \bar{y}_1(0) = 0.01$ and $\phi_1(0) = \phi_2(0) = 0.01$, for $\bar{\omega} > 1$, they never depart very far from their equilibrium positions. Therefore, the motion is said to be stable above critical speed at least for $\beta' = 3.8$. Figure 11 shows a plot of $\phi_1(\bar{t})$ versus dimensionless time

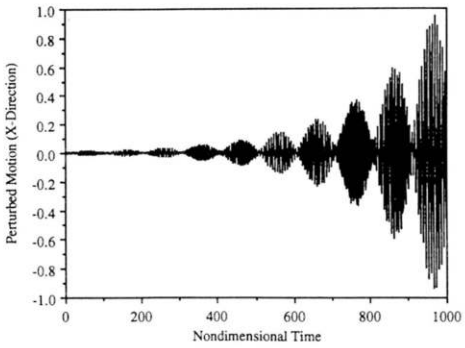

FIGURE 12 X-direction perturbation versus nondimensional time ($\bar{\omega} = 1.0$). Initial conditions: $\bar{x}_o(0) = \bar{y}_o(0) = 0.01$, $\dot{\bar{x}}_o(0) = \dot{\bar{y}}_o(0) = 0$, $\phi_{s1} = 3.13$, $\phi_{s2} = 3.15$, $\phi_1(0) = \phi_2(0) = 0.01$, $\dot{\phi}_1(0) = \dot{\phi}_2(0) = 0$, $\bar{m} = 0.005$, $\bar{R} = 0.001$, and $\beta' = .01$.

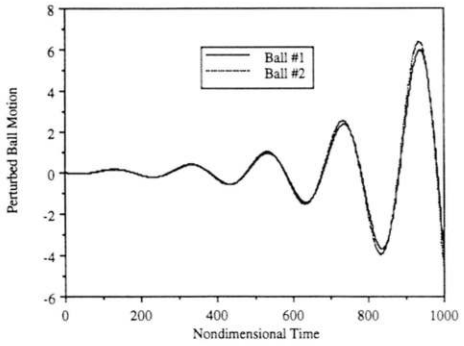

FIGURE 13 Perturbed ball motion versus nondimensional time ($\tilde{\omega} = 1.0$). Initial conditions: $\tilde{x}_o(0) = \tilde{y}_o(0) = 0.01$, $\dot{\tilde{x}}_o(0) = \dot{\tilde{y}}_o(0) = 0$, $\phi_{s1} = 3.13$, $\phi_{s2} = 3.15$, $\phi_1(0) = \phi_2(0) = 0.01$, $\dot{\phi}_1(0) = \dot{\phi}_2(0) = 0$, $\tilde{m} = 0.005$, $\tilde{R} = 0.001$, and $\beta' = .01$.

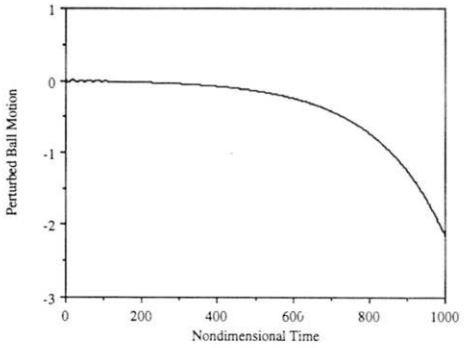

FIGURE 15 Perturbed ball motion versus nondimensional time ($\tilde{\omega} = 0.7$). Initial conditions: $\tilde{x}_o(0) = \tilde{y}_o(0) = 0.01$, $\dot{\tilde{x}}_o(0) = \dot{\tilde{y}}_o(0) = 0$, $\phi_{s1} = 3.13$, $\phi_{s2} = 3.15$, $\phi_1(0) = \phi_2(0) = 0.01$, $\dot{\phi}_1(0) = \dot{\phi}_2(0) = 0$, $\tilde{m} = 0.005$, $\tilde{R} = 0.001$, and $\beta' = .01$.

with increased initial motions of $\phi_1(0) = \phi_2(0) = 0.5$ (28.65°). From this figure even if the balls are initially located far from the equilibrium positions, the two balls come back to the equilibrium positions. From Figs. 12–15 even if the balls are initially located at the dynamic equilibrium positions, at critical speed and below critical speed, they do not remain in those positions. Therefore, the motion is said to be unstable at critical speed and below critical speed.

CONCLUSIONS

From the preceding work, the following conclusions were drawn. The equations of motion of the balls were derived by the Lagrangian method. Steady solutions were derived from the analytic model. Perturbation solutions were also obtained from the analytic model. To investigate dynamic stability of the perturbed motion, numerical simulation of the Floquet algorithm with only one ball and direct computer simulation were conducted. Based on the results of stability investigation, ball positions that result in a balanced system are stable above the critical speed for $\beta' > 3.8$. At critical speed the perturbed motion is said to be stable for $\beta' > 23$. However, the system is unstable below critical speed in any case of β'. However, further study of this self-compensating dynamic balancer for a nonuniform rotating system with variable rotating speed and the effect of β' on dynamic stability for multiple balls should be done.

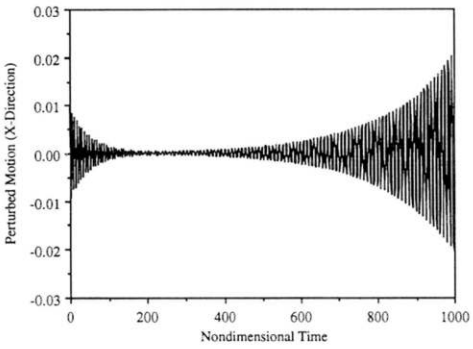

FIGURE 14 X-direction perturbation versus nondimensional time ($\tilde{\omega} = 0.7$). Initial conditions: $\tilde{x}_o(0) = \tilde{y}_o(0) = 0.01$, $\dot{\tilde{x}}_o(0) = \dot{\tilde{y}}_o(0) = 0$, $\phi_{s1} = 3.13$, $\phi_{s2} = 3.15$, $\phi_1(0) = \phi_2(0) = 0.01$, $\dot{\phi}_1(0) = \dot{\phi}_2(0) = 0$, $\tilde{m} = 0.005$, $\tilde{R} = 0.001$, and $\beta' = .01$.

REFERENCES

Alexander, J. D., 1964, "An Automatic Dynamic Balancer," *Proceedings of the 2nd Southeastern Conference,* Georgia Institute of Technology, Vol. 2, pp. 415–426.

Darlow, M. S., 1989, *Balancing of High-Speed Machinery,* Springer–Verlag, New York.

Hahn, W., 1967, *Stability of Motion,* Springer–Verlag, New York.

Lee, Jongkil, 1993, *Theoretical and Experimental Analysis of Self-Compensating Dynamic Balancer in a Rotating Mechanism,* Ph.D. Dissertation, University of Utah, Salt Lake City.

Nayfeh, A. H., and Mook, D. T., 1979, *Nonlinear Oscillations,* John Wiley & Sons, New York.